

nm23-H1 mutation in neuroblastoma

SIR—Reduced expression of *nm23-H1*, which encodes the nucleoside diphosphate kinase A (ref. 1), is associated with a high potential for metastasis in some tumour types², but its expression is increased in aggressive neuroblastoma, a childhood tumour of variable outcome³. To investigate the role of *nm23-H1* in neuroblastoma, we looked for mutations in this gene in 24 primary neuroblastoma tumours at different stages of the disease using the polymerase chain reaction (PCR) combined with analysis by single-stranded conformation polymorphism (SSCP)⁴ and Southern blotting.

Three sets of primers covering the coding sequence of *nm23-H1* were used separately for PCR amplification of complementary DNA prepared by reverse transcription of tumour poly(A)⁺ RNA. Four tumours from patients with advanced disease (stages 3 and 4)⁵ gave an altered DNA conformation on SSCP analysis when the primers used for PCR encompassed nucleotides 211 to 502 (Fig. 1). All four tumours gave rise to the same band and a less intense neighbouring normal band.

We used cDNA from two of the four

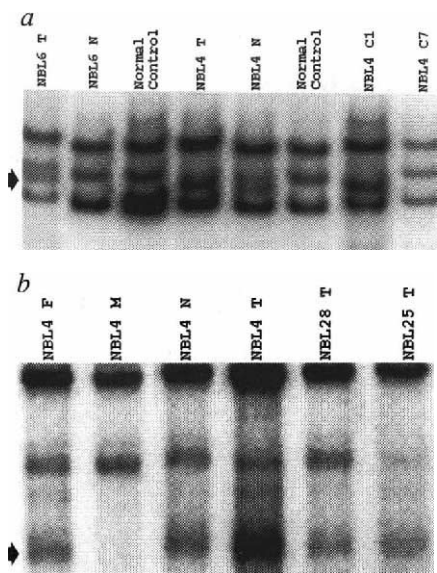


FIG. 1 PCR-SSCP analysis of *nm23-H1* cDNA prepared from tumour (T) and non-tumour (N) tissue from patients with neuroblastoma (NBL). cDNA was also prepared from peripheral blood lymphocytes obtained from normal control subjects and from the father (F) and mother (M) of NBL4. The variant band is indicated by an arrow. Patterns are shown for individual cDNA clones (C1 and C7) prepared from NBL4 tumour tissue. *a*, Samples were denatured and loaded onto a 6% polyacrylamide gel containing 10% glycerol, 90 mM Tris-borate, pH 8.3, and 4 mM EDTA⁴. Alternatively, in *b*, samples were run on a 0.5 X HydroLink mutation-detection enhancement gel.

tumours to generate cDNA clones which we analysed individually by SSCP: each clone gave either the variant band or the normal neighbouring band (Fig. 1*a*). When we sequenced the clones with altered conformation from these two tumours, we discovered an A-to-G nucleotide change in the coding region of *nm23-H1*, which resulted in a substitution by glycine for serine at position 120. This nucleotide swap creates a new cutting site for the restriction enzyme *HphI*, so the mutation can be readily detected.

From the four tumours giving an altered conformation by SSCP analysis, a new, smaller band (109 base pairs) was evident in *HphI*-digested cDNA which was not seen in cDNA from normal individuals; this band was the same size as the fragment resulting from the extra *HphI* restriction site created by the substitution (Fig. 2). When we screened cDNA from 64 normal individuals for the Ser 120 → Gly substitution using PCR-SSCP and *HphI* restriction analysis, we found normal patterns in all 64 samples.

Non-tumour tissue was available for two of the four patients whose tumour contained the Ser 120 → Gly substitution. One patient (NBL6) gave no abnormal bands from normal tissue (Fig. 1), indicating that the substitution was probably a result of a somatically acquired mutation; another (NBL4) had roughly equal amounts of normal and variant *nm23-H1* in cDNA from normal tissue (Fig. 1). Evidence for inheritance of a variant allele in patient NBL4 was obtained by SSCP analysis of cDNA from the parents. The father's, but not the mother's, cDNA had the same altered conformation as that from NBL4's normal tissue (Fig. 1*b*).

There was a small increase in *nm23-H1* gene copy number in 4 of the 24 primary tumours, based on phosphorimaging of Southern blots⁶. All four tumours were from patients with advanced disease. The highest gene copy number (10 copies) was found in NBL4's tumour with the inherited Ser 120 → Gly substitution. This tumour carried predominantly the form of *nm23-H1* with the substitution (Fig. 1). Southern blot analysis of the *nm23-H2* gene, which has been mapped to the same region (17q21) as *nm23-H1* (ref. 7), showed no evidence of increased *nm23-H2* gene copy number in any of the neuroblastoma tumours.

We confirmed that the substitution was a somatically acquired mutation in the case of NBL6, using two oligonucleotide primers for PCR amplification of a 123-base-pair genomic fragment spanning this substitution at nucleotide 442. *HphI* digestion of the PCR product from normal tissue showed that an A-to-G substitution was present at position 442, giving a

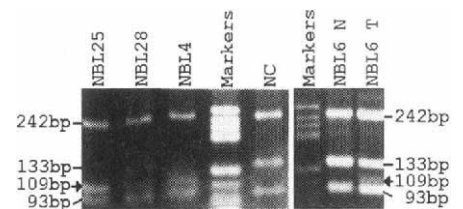


FIG. 2 *HphI* digestion of *nm23-H1* cDNA from the four tumours giving the same altered band by SSCP, and of non-tumour tissue (N) for NBL6 and a normal control (NC). The A-to-G substitution at position 442 creates an additional *HphI* digestion site in a 133-base-pair (bp) fragment which results in 109-bp (arrow) and 24-bp fragments. The 133-bp fragment is seen in the control and is faint or absent in NBL25, 28, 4 and 6.

75-base-pair fragment for NBL4 but no fragment for NBL6; the conclusion was the same when the 123-base-pair PCR-amplified genomic fragments were analysed by SSCP. This substitution must therefore be inherited in the case of NBL4 and a somatic mutation in the case of NBL6.

Genomic material was also analysed for an additional group of 26 neuroblastoma patients for whom paraffin-embedded tissue blocks were available⁸. DNA from two of 14 patients with advanced neuroblastoma showed altered bands attributable to the A-to-G substitution in their tumour, but not in normal tissue. None of 12 tumours from patients with limited-stage neuroblastoma showed evidence of this substitution. Genomic DNA from 36 normal individuals lacking this substitution in their cDNA, from 26 breast carcinomas and 17 acute leukaemias was also examined by *HphI* digestion of the amplified 123-base-pair fragment. No A-to-G substitution was detected in this group of 79 samples, excluding the possibility that this substitution represents a common polymorphism.

Our results show that a Ser 120 → Gly substitution is present in 6 of 28 advanced tumours but not in any of 22 limited-stage tumours, indicating that the mutation could be a feature of advanced neuroblastoma. We will show elsewhere that the mutant enzyme identified here still retains its catalytic activity but is more susceptible to denaturation, like the conditional lethal nucleoside diphosphate kinase mutation

- Gilles, A.-M., Presecan, E., Vonica, A. & Lascau, I. *J. Biol. Chem.* **266**, 8784–8789 (1991).
- Rosengard, A. M. *et al. Nature* **342**, 177–180 (1989).
- Hailat, N. *et al. J. Clin. Invest.* **88**, 341–345 (1991).
- Orita, M., Suzuki, Y., Sekiya, T. & Hayashi, K. *Genomics* **5**, 874–879 (1989).
- Evans, A. E., D'Angio, G. J. & Randolph, J. A. *Cancer* **27**, 374–378 (1971).
- Johnston, R. F., Pickett, S. C. & Barker, D. L. *Electrophoresis* **11**, 355–360 (1990).
- Backer, J. M. *et al. Oncogene* **8**, 497–502 (1993).
- Innis, M. A., Gelfand, D. H., Sninsky, J. J. & Thomas, J. W. *PCR Protocols: A Guide to Methods and Applications* (Academic, San Diego, 1990).
- Dearolf, C. R., Tripoulos, N., Biggs, J. & Shearn, A. *Dev. Biol.* **129**, 169–178 (1988).
- Lascau, I., Chaffotte, A., Limbourg-Bouchon, B. & Veron, M. *J. Biol. Chem.* **267**, 12775–12781 (1992).

Killer of Prune in *Drosophila melanogaster*^{9,10}. The effects of the *nm23-H1* gene in tumour progression and metastasis probably depend on both its level of expression and the occurrence of specific mutations in its protein.

Christina L. Chang, Xiao-xiang Zhu, Didier H. Thoraval, David Ungar, Jawhar Rawwas, Nivedita Hora, John R. Strahler, Samir M. Hanash

Department of Pediatrics,

Eric Radany

Department of Radiation Oncology,
University of Michigan School of Medicine,
R4451 Kresge I, Box 0510,
Ann Arbor,
Michigan 48109, USA

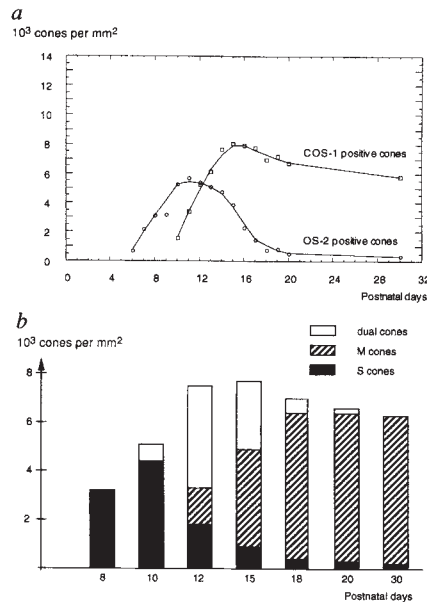
Retinal cone differentiation

SIR — During retinal development, differentiation of each cell type follows a strict timetable: in rodent retinae^{1,2} the short-wave-sensitive cone photoreceptor molecule (S pigment) is expressed before the middle-wave-sensitive (M) cone pigment, and we now show that this appearance of M cones after the S cones is a result of their development from S cones. So S-pigment expression must be the default pathway in cone differentiation, with prospective M cones switching to the green-sensitive pathway only secondarily in response to an as yet unknown factor.

We followed the kinetics of expression of S and M cones in the developing rat and gerbil retina with OS-2 and COS-1, antibodies specific for the carboxyl terminus of the S and M pigments, respectively³. In the rat, immunopositive S cones started to appear on the fifth postnatal day (P5) and their density increased until P11; the first COS-1-positive M cones emerged at P9, and reached the maximum density at P15 (see *a* in figure). The number of the OS-2-positive cones then dropped by almost 95 per cent, whereas COS-1-positive cones decreased only slightly.

This sudden drop in the S-cone forerunners coinciding with the accumulation of M cones indicated that the S cones might be changing phenotype and transforming into M cones rather than dying out. Although programmed cell death probably influences adult patterns, we saw no degenerating or dying cones during the critical period of cone development, making this an unlikely explanation for the fall in S cones. Neither can it be accounted for by the roughly ten per cent expansion of the retinal surface between P10 and P30, nor by the lateral movement of cones during morphogenesis, as both cone types are uniformly distributed across the entire retina at all ages.

Owing to the rapid randomization of newly synthesized outer-segment proteins

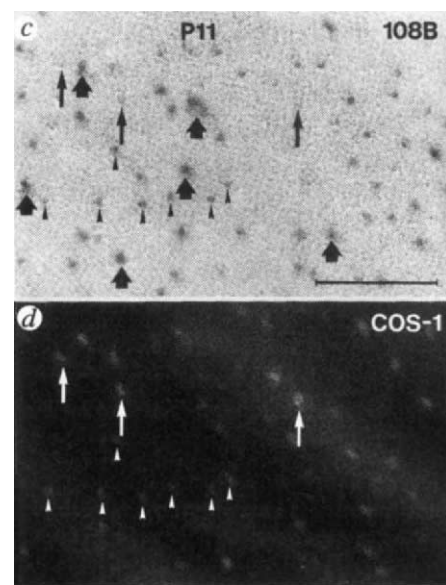


a, Quantitative analysis of cone development in rat retinae. OS-2- and COS-1-positive cones were counted on unit (0.1 mm²) areas and plotted as a function of postnatal time. The bound antibodies were detected with rhodamine and fluorescein isothiocyanate (TRITC and FITC, respectively). Topographically identical areas, located halfway between the optic nerve head and the superior edge of the ora serrata, were selected for comparison. Mean values derived from three animals of the same age were used. Cones expressing S pigment appear earlier (OS-2, circles), but after reaching their peak, the curve drops steeply. M-pigment-containing cones emerge later (COS-1, squares), and after peaking, the curve declines only slightly to plateau just below the maximum. *b*, Diagram showing the densities of cones stained with either 108B, a rabbit polyclonal antibody raised against a C-terminal epitope of the human blue visual pigment⁶ (S cones), or COS-1 (M cones), or both (dual cones). Bound antibodies were detected with FITC and TRITC, respectively, on double-labelled rat retinae. Note that dual cones arise during only a short period of the development. Samples shown are from identical areas of individual retinae, but the entire retina contained the same distribution of differently stained cones at each age. *c*, *d*, Double immunolabel of an 11-day-old rat retina with 108B and COS-1. Bound antibodies were detected by diaminobenzidine (108B) and FITC (COS-1). Pairs of photographs were taken from the same retinal area using Nomarski optics (*c*) and a fluorescent filter (*d*). Cones are mostly stained with both antibodies (arrowheads). There are a few heavily labelled 108B cones (genuine S cones) that are not recognized by COS-1 at all (thick arrows). Cones strongly labelled by COS-1 generally bind 108B only weakly (thin arrows). Scale bar, 25 μ m.

and the much slower shedding of the apical disks^{4,5}, cones containing both pigments should be evident during the proposed shift. We used double-label immunocytochemistry to test for such cones in the rat and gerbil, by reacting whole retinae with 108B, an antibody against human blue opsin⁶, and with the M-cone-specific COS-1; bound antibodies were detected using different fluorochromes or with diaminobenzidine and fluorochrome. We also reacted consecutive tangential sections alternately with OS-2 and COS-1 to identify with both pigments (not shown). OS-2- and 108B-labelled photoreceptors are known to be identical⁷.

Between P9 and P20, many cones bound both antibodies (*b* in figure), indicating the temporary coexistence of both pigments. Initially, all cones were recognized exclusively by S-pigment-specific antibodies. Later, the majority of cones were seen to be at various stages of transition between the two phenotypes (*c* and *d*). By P30 most of these cones were undetected by 108B and OS-2 and only a few, genuine S cones retained the original phenotype.

Our results show that most of the early-maturing S cones in the rat and gerbil



retina change their phenotype to become M cones. The green-sensitive cones thus derive from the transforming cones, while a few cones do not undergo the shift and constitute the definitive S-cone population. The differentiation around the second postnatal week indicates that instead of colour-specificities being pre-determined, the ultimate cone phenotypes will be defined only after the onset of visual pigment synthesis.

Ágoston Széi*

Theo van Veen

Department of Zoology,
University of Gothenburg,
Gothenburg, S-41390,
Sweden

Pál Röhlich

Laboratory of Electron Microscopy,
Semmelweis University Medical School,
Budapest, H-1450, Hungary

* At both addresses.

- Wang, Y. *et al.* *Neuron* **9**, 429–440 (1992).
- Széi, Á., Röhlich, P., Mieziewska, M., Aguirre, G. & van Veen, T. J. *comp. Neurol.* **331**, 564–577 (1993).
- Röhlich, P. & Széi, Á. *Curr. Eye Res.* **12**, 935–944 (1993).
- Young, R. W. *Invest. Ophthalmol.* **15**, 700–725 (1976).
- Bok, D. *Invest. Ophthalmol. vis. Sci.* **26**, 1659–1694 (1985).
- Lerea, C. L., Bunt-Milam, A. H. & Hurley, J. B. *Neuron* **3**, 367–376 (1989).
- Széi, Á. *et al.* *J. comp. Neurol.* **325**, 327–342 (1992).